

Contrastive Learning of Image Representations with Cross-Video Cycle-Consistency

Haiping Wu
McGill University, Mila

Xiaolong Wang
UC San Diego

Abstract

Recent works have advanced the performance of self-supervised representation learning by a large margin. The core among these methods is intra-image invariance learning. Two different transformations of one image instance are considered as a positive sample pair, where various tasks are designed to learn invariant representations by comparing the pair. Analogically, for video data, representations of frames from the same video are trained to be closer than frames from other videos, i.e. intra-video invariance. However, cross-video relation has barely been explored for visual representation learning. Unlike intra-video invariance, ground-truth labels of cross-video relation is usually unavailable without human labors. In this paper, we propose a novel contrastive learning method which explores the cross-video relation by using cycle-consistency for general image representation learning. This allows to collect positive sample pairs across different video instances, which we hypothesize will lead to higher-level semantics. We validate our method by transferring our image representation to multiple downstream tasks including visual object tracking, image classification, and action recognition. We show significant improvement over state-of-the-art contrastive learning methods. Project page is available at https://happywu.github.io/cycle_contrast_video.

1. Introduction

There has been a surge of recent interest in contrastive learning of visual representation [65, 29, 3, 28, 56, 9, 26, 40]. We have witnessed that contrastive learning outperforms supervised pre-training with large-scale human annotations in various visual recognition tasks [26, 9]. The key of this self-supervised task is to construct different views and transformations of the same instance, and learn the deep representation to be invariant to the view changes. To construct different views for forming positive image pairs in contrastive learning, the most common way is to use different data augmentations on the same instance (e.g.

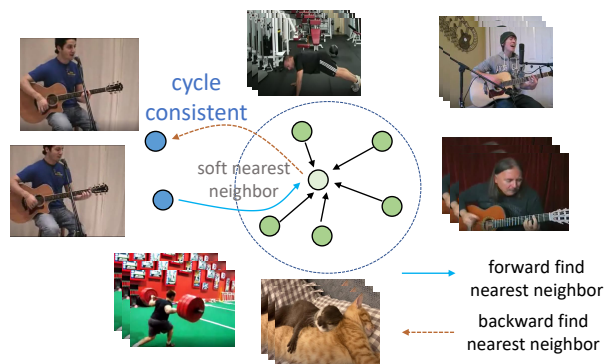


Figure 1: Cross-video cycle-consistency for image representation learning. Starting from one frame in a video, we find its soft nearest neighbor from other videos as a forward step, then the cycle-consistency is achieved when the soft nearest neighbor finds its closest frame within the same video as the start frame in a backward step.

random cropping, image rotation, colorization).

However, simply performing artificial augmentation on single instance has shown its limitation in multiple applications [57, 66]. For example, Tian *et al.* [57] have performed detailed analysis on how different augmentations can affect different downstream visual recognition tasks. Going beyond single image, researchers have also looked into videos as the source for obtaining positive pairs of training images [48, 21, 60]. That is, two nearby frames in the same video can be taken as a natural augmentation in time for the same object instance. By training using temporal augmentation, the representation can learn viewpoint and deformation invariance. However, these approaches are still limited to find positive pairs and learning their similarity within a single instance.

In this paper, we propose to perform contrastive learning with positive image pairs sampled across different videos instead of the same video. We hypothesize this can potentially capture higher-level semantics and categorical information beyond low-level intra-instance invariances modeled by previous approaches. Specifically, given two image

frames I_i and I_j from a video, instead of directly using them as a positive pair for training [48, 21], we will first “explain” frame I_i by composing frames from other videos that are similar to I_i , then compare the composed frames to I_j for contrastive learning.

Assuming we have a neural network feature extractor to learn, we extract the feature representations for the image frame I_i as q_i , and representations for frames from other videos as $U = \{u_1, u_2, \dots, u_m\}$. Given these representations, we compute the similarities between q_i and U , and normalize them to a probability distribution. We use this probability distribution to re-weight and compose the features U as a new feature representation for frame I_i (frames that are more similar to I_i will have larger weight). We call this new feature as a soft nearest neighbor to I_i . We then form a positive pair of training data with this new representation and the feature of I_j (a different frame from the same video as I_i). As shown in Figure 1, this procedure goes through a cycle of starting from one frame I_i in a video, searching forward by matching frames from other videos, and retrieving frame I_j backward in the first video. We call this process *Cycle-Consistent Contrastive Learning*. Intuitively, enforcing such a cycle-consistency can explicitly push video frames with similar structure closer, thus leads to a natural clustering of semantics.

We perform the proposed self-supervised representation learning on unlabeled video dataset Random Related Video Views (R2V2) [21] and transfer the learned representation to various downstream tasks including visual object tracking, image classification and action recognition. We stress our goal is to use the temporal signal to learn a **general image-level representation** for multiple applications beyond videos-level recognition tasks. We show significant improvements over multiple state-of-the-art approaches. We also conduct extensive ablation studies of different components and design choices of our method.

Our contributions include: (i) A novel cross-video cycle-consistent contrastive learning objective that explores cross-video relations, going beyond previous intra-image and intra-video invariant learning; (ii) The proposed loss enforces image representations from the same category (of similar visual structures) closer without explicitly generating pseudo labels; (iii) The learned image representation achieves significant improvement in multiple downstream tasks including object tracking, image classification and action recognition.

2. Related Work

Contrastive learning. The self-supervised contrastive learning methods [23, 16, 65, 29, 44, 3, 28, 56, 78, 9, 26, 40, 10, 8] try to learn image representations under different transformations agree by forming positive and negative pairs, and make the representations of positive pairs have

high similarity and negative pairs have low similarity. The typical way of generating positive pairs is performing artificial data augmentations on a single image instance. For example, Chen *et al.* [9] introduce a contrastive learning baseline with different types of augmentations, including random cropping, resizing, color distortion, gaussian blur, *etc.* He *et al.* [26] proposes MoCo which introduces a momentum network to encode a queue of a large number of negative samples for efficient learning. In this work, we build our model based on the MoCo framework. However, instead of learning with positive pairs by augmenting the same image, we propose a new objective which finds positive pairs of sample across videos for contrastive learning of image representations.

Self-supervised image representation learning from videos. Going beyond learning from a single image [15, 13, 47, 14, 72, 19], video naturally offers temporal information and multi viewpoints for objects, which have been extensively utilized as self-supervisory signals in representation learning [22, 1, 33, 60, 46, 45, 41, 61, 39, 7, 63, 35, 51]. For example, Wang and Gupta [60] use tracking to provide supervision signals that makes the feature representations of tracked patches similar. Recent works [21, 48, 32, 68] further extend similarity learning between video frames under the contrastive learning framework, where the positive pairs for training are frames sampled from the same video. It has been shown image representations with viewpoint invariance can be learned. Our work is motivated by these previous works, and going beyond viewpoint invariance, learning using positive pairs across videos can potentially lead to image representations with higher-level semantics. While contrastive learning has also been applied to video representation learning with 3D ConvNets for action recognition [35, 24, 36, 5, 50, 58, 25, 34, 42], we emphasize our work is focusing on learning a general image representation for multiple tasks beyond action recognition including visual tracking and image classification.

Cycle-consistency learning. Our work is influenced by cycle-consistency learning in different computer vision applications including 3D scene understanding [31, 73, 20, 71], image alignment and translation [74, 76, 75, 77], and space-time alignment in videos [4, 62, 38, 17, 59, 32, 49, 37]. For example, Wang *et al.* [62] propose to perform forward and backward tracking in time to achieve a cycle-consistency for learning temporal correspondence. Dwivedi *et al.* [17] formulates a temporal cycle consistency loss which aligns frames from one video to another between a pair of videos, and achieves good performance in video frame alignment tasks. Building on these two works, Purushwalkam *et al.* [49] propose to track object patches inside a video and align them across videos at the same time. While these results are encouraging, both approaches learning from video pairs [17, 49] require human annota-

tors to provide ground-truth pairs (video-level) in training with a small scale of videos. In this paper, we propose to go beyond these restrictions, and apply cross-video cycle-consistency learning without any human annotations. These not only allows learning with a large-scale videos, but also generalizes our representations to multiple downstream vision tasks.

3. Cycle-Consistent Contrastive Learning

In this section, we first introduce contrastive learning with different forms of invariant learning targets. Then we propose our method with cross-video cycle-consistency learning.

3.1. Intra-Image and Intra-Video Invariance

The core of self-supervised contrastive learning [26, 9] is to learn representations which maximize the agreement between different views, augmentations of one image instance, and minimize the similarity between two different and unrelated instances at the same time. Most methods share the similar learning objective, which is to make the representations *intra-image* invariant. We describe the formulation of the objective as follows.

Given an query image I_i , the feature extractor encodes it to feature representations q_i and k_i under two different data augmentations. The intra-image invariance learning considers q_i and k_i as an a positive training pair and minimizes their representation distance, while maximizing the representation distance of q_i and a set of negatives $U = \{u_1, u_2, \dots, u_m\}$, which is a set of feature representations extracted from different images. The intra-image invariance contrastive learning loss function is defined as,

$$\mathcal{L}_{\text{intra-image}} = -\log \frac{\exp(\text{sim}(q_i, k_i) / \tau)}{\sum_{u \in \{U, k_i\}} \exp(\text{sim}(q_i, u) / \tau)}, \quad (1)$$

where τ is the temperature constant and $\text{sim}(x, y) = x^\top y / \|x\| \|y\|$ is the cosine similarity between two feature vectors. The loss function tries to classify q_i is similar to k_i from the same image against features in U from different images, achieving the intra-image invariance learning.

While intra-image invariance learning gives us good representations, augmentations of static images fail to capture viewpoint and deformation variations of instances (e.g. different viewpoints or gestures of one person) [48]. It is natural to resort to sequential video data that has variations of the same instance across time, extending the *intra-image* invariance learning to *intra-video* invariance learning. The intra-video invariance learning considers frames within the same video in a local time window as a invariant set to form positive pairs in training [52, 21, 48]. Similarly to Eq. 1, the

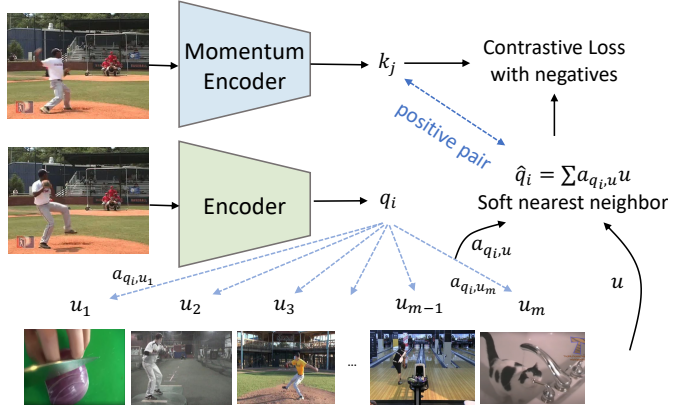


Figure 2: The pipeline for the proposed cross-video cycle-consistency loss $\mathcal{L}_{\text{cycle}}$. $U = \{u_1, u_2, \dots, u_m\}$ is the neighbor representation set. Given the query feature q_i , we construct its soft nearest neighbor \hat{q}_i by combining frame information from other videos. We use the key feature k_j from the same video and \hat{q}_i as a positive pair for contrastive learning.

intra-video invariance contrastive learning loss is defined as,

$$\mathcal{L}_{\text{intra-video}} = -\log \frac{\exp(\text{sim}(q_i, k_j) / \tau)}{\sum_{u \in \{U, k_j\}} \exp(\text{sim}(q_i, u) / \tau)}, \quad (2)$$

where k_j is the feature representation of image I_j , which is sampled from the same video of I_i . $\mathcal{L}_{\text{intra-video}}$ tries to make the feature representations of images from the same video closer than images from different videos. When the sampled image I_j is the same as I_i , $\mathcal{L}_{\text{intra-video}}$ is identical to $\mathcal{L}_{\text{intra-image}}$. We can see the intra-image invariance learning as a special case of the intra-video invariance learning.

3.2. Cross-Video Cycle-Consistency Objective

Both intra-image and intra-video invariance learning make the feature representations of the same instance (from the same image or video) closer. However, there is no explicit regularization on the distances between representations from the same class (or images of similar visual structures). For instance, the representations of different cat instances should be close and representations of frames from different videos on playing tennis should also be similar. In this section, we propose to find cross-video correspondence with cycle-consistency without using any ground-truth labels, and incorporate the correspondence in contrastive learning. The pipeline of the new proposed objective is shown in Figure 2 and we will introduce the formulations as following.

Our new objective consists of a forward and a backward nearest neighbor processes. Given an encoded query feature representation q_i of I_i from a video V , we first compute its nearest neighbor \hat{q}_i in a candidate set U containing frames from any videos. Then, we find the nearest neighbor of \hat{q}_i

backwards within the union set of U and V . We emphasize that U *does not* include any frames from the video V . The cycle-consistency is achieved when the backward nearest neighbor of \hat{q}_i is in the desired invariance learning set of q_i from V . In order to make the learning differentiable, we propose to compute the soft nearest neighbor as the *forward step* in our objective. Formally, the soft nearest neighbor \hat{q}_i of q_i in $U = \{u_1, u_2, \dots, u_m\}$ is calculated as,

$$\hat{q}_i = \sum_{u \in U} \alpha_{q_i, u} u, \quad (3)$$

where $\alpha_{q_i, u}$ is the normalized similarity of q_i and u , which is defined as

$$\alpha_{q_i, u} = \frac{\exp(\text{sim}(q_i, u)/\tau)}{\sum_{u' \in U} \exp(\text{sim}(q_i, u')/\tau)}, \quad (4)$$

where τ is the temperature and $\text{sim}(x, y) = x^\top y / \|x\| \|y\|$ is the cosine similarity.

Given the soft nearest neighbor \hat{q}_i , we assume if a representation is good for understanding the high-level semantics, \hat{q}_i should be in the invariance set of q_i . Recall that we denote the invariance target of q_i as k_j (feature of a different frame in the same video) in intra-video invariance learning. We perform non-parametric classification as the *backward step*, and the cross-video cycle contrastive loss is defined as,

$$\mathcal{L}_{\text{cycle}} = -\log \frac{\exp(\text{sim}(\hat{q}_i, k_j)/\tau)}{\sum_{u \in \{U, k_j\}} \exp(\text{sim}(\hat{q}_i, u)/\tau)}, \quad (5)$$

where k_j is the feature representation of image I_j from the invariant set of I_i , and we consider I_j and I_i are sampled from the same video V .

Intuitively, Eq. 3 tries to use the representations in the candidate set to reconstruct the query feature representation, according to the similarity measurement of Eq. 4. Then $\mathcal{L}_{\text{cycle}}$ is minimized when the reconstructed feature representation is close to the representations of another image from video V . In this way, the model will learn to find correspondence across videos where images with similar visual structures are encouraged to be the same, and invariant within a video at the same time. By building the correspondence across videos, it can potentially help the representations to learn category-level information.

The overall learning target is a combination of intra-video invariant loss $\mathcal{L}_{\text{intra-video}}$ and cross-video cycle consistency loss $\mathcal{L}_{\text{cycle}}$, defined as

$$\mathcal{L} = \mathcal{L}_{\text{intra-video}} + \lambda \mathcal{L}_{\text{cycle}}, \quad (6)$$

where λ is a balancing factor of the two learning targets. We will provide ablation on λ in our experiments.

Algorithm 1 Pseudocode for $\mathcal{L}_{\text{cycle}}$, PyTorch-like

```
# f_q: encoder + projection mlp
# f_k: momentum encoder + projection mlp
# mon: momentum parameter
# queue: key dictionary (c x K)
# m: size of neighbor set
# t: temperature

f_k.params = f_q.params

for x_i, x_j in loader: # load a minibatch with n
    samples, each sample contains two randomly
    selected frames from one video
    x_i, x_j = aug(x_i), aug(x_j) # random augmentation
    q_i, k_j = f_q(x_i), f_k(x_j) # feature extraction,
    n x c
    k_j = k_j.detach()

    u = random.choice(queue, m) # randomly select
    neighbor set
    r_queue = queue \ u # get remain elements of queue
    a = softmax(cos_similarity(q_i, u)/t) # calculate
    similarity: n x m
    soft_nn = matmul(a, u) # get soft nearest neighbor

    logits = matmul(soft_nn, cat([k_j.T, r_queue], dim
    =1))
    labels = zeros(n)
    cycle_loss = CrossEntropyLoss(logits/t, labels) #
    calculate cycle back classification loss

    enqueue(queue, k_j)
    dequeue(queue)
```

matmul: matrix multiplication; cat: concatenation.

Implementation details for neighbor set U . In our experiments, we use two separate nearest neighbor sets for *forward and backward steps* for our objective $\mathcal{L}_{\text{cycle}}$. The nearest neighbor set U in Eq. 3 is selected by randomly sampling from the current memory bank [26] at each training iteration. The remaining elements in the memory bank are used as negative candidates for finding the nearest neighbor backwards in Eq. 5. We provide the pseudo code of the $\mathcal{L}_{\text{cycle}}$ in Alg. 1.

4. Experiments

In this section, we conduct experiments to perform unsupervised representation learning using the proposed learning objectives. We show that the learned representation transfer well to various downstream tasks. Then we design extensive ablation experiments to study the effectiveness of the proposed cross-video cycle-consistent learning method.

4.1. Experiments settings

Dataset . We perform unsupervised representation learning on Random Related Video Views (R2V2) [21] dataset, which is a large-scale diverse video frames collection. It has 2.7M videos, with 4 frames for each video. For smaller models and ablation studies, we use a subset of it for time efficient, which has 109k videos and 438k frames in total, which we refer as R2V2-S.

Network Architecture . ResNet-18 [27] is used as backbone for major ablation studies for its efficiency and ac-

Method	Backbone	Dataset	OTB	
			Precision	Success
Supervised [27]	ResNet-18	ImageNet	61.4	43.0
SimSiam [11]	ResNet-18	ImageNet	58.8	42.9
MoCo [26]	ResNet-18	ImageNet	62.0	47.0
VINCE [21]	ResNet-18	R2V2	62.9	46.5
Ours	ResNet-18	R2V2-S	65.6	48.6
Supervised [27]	ResNet-50	ImageNet	65.8	45.5
SimSiam [11]	ResNet-50	ImageNet	61.0	43.2
MoCo [26]	ResNet-50	ImageNet	63.7	46.5
SeCo* [70]	ResNet-50	Kinetics	71.9	51.8
VINCE [21]	ResNet-50	R2V2	40.2	30.0
Ours	ResNet-50	R2V2	69.3	49.2

Table 1: Visual Object Tracking performance on OTB-100 compared with other unsupervised representation pretrain methods. SiamFC with one additional 1x1 convolution is added. Note that concurrent work SeCo* uses two-stage training strategy, where it uses MoCo pretrained on ImageNet as first stage.

curacy. One fully connected layer (512 x 64) is used as projection layer after the global average pooling layer to obtain the embedding features. ResNet-50 is also adapted for comparing with other methods. Following the study in [66], $\mathcal{L}_{\text{intra-video}}$ and $\mathcal{L}_{\text{cycle}}$ use separate projection layers as they have different invariance learning targets. Following MoCo [26], we use a query encoder network f_q and a key encoder network f_k , where the parameters θ_k of f_k is updated by the parameters θ_q of f_q , using $\theta_k \leftarrow m\theta_k + (1 - m)\theta_q$. The momentum coefficient m is set to 0.999 and the memory bank size for classification is 65536. The temperature τ is set to 0.07.

Training. We use SGD to optimize the unsupervised representation learning for a total of 200 epochs. The mini-batch size is 256 in 8 GPUs. The initial learning rate is 0.06. Other training recipes follow [26].

4.2. Transfer to visual object tracking

We perform object tracking on the learned representations. SiamFc [6] is used as tracking method, which consists of one 1x1 convolution upon the pre-trained frozen representations. The training is performed on GOT-10k [30] dataset and we test it on OTB2015 [64]. The results are shown in Table 1. As we could see, when using ResNet-18 as backbone, our method outperforms previous unsupervised representation methods, as well as ImageNet supervised one, obtaining 65.6 precision, an 2.7 improvement over VINCE [21], which trains on the same dataset. Our method also surpasses previous contrastive learning methods when using ResNet-50 as backbone, and achieves 3.5 precision improvement over ImageNet supervised pretrain model. Note that we observed a performance drop when using intra-image objective alone when switching from ResNet-18 to ResNet-50. This also occurred in VINCE [21] which uses the same dataset for pretraining. We conjure

Invariance			Backbone	OTB	
intra image	intra video	cross video		Precision	Success
✓			ResNet-18	53.7	41.2
✓	✓		ResNet-18	60.1	45.5
✓	✓	✓	ResNet-18	65.6	48.6
✓			ResNet-50	47.4	34.4
✓	✓		ResNet-50	68.4	48.9
✓	✓	✓	ResNet-50	69.3	49.2

Table 2: Ablation of different losses components (invariance target) for OTB-100 tracking on frozen features. Representations are pretrained on R2V2-S with ResNet-18, and R2V2 with ResNet-50. We clearly see that our proposed method with cross-video cycle consistency learning target achieves the best performance.

that it is because there are only 4 frames per video, covering a long temporal window, making it hard to find correspondence within the same video, which is important for tracking task. Although our method is slightly inferior to SeCo [70]. However, SeCo utilizes a two-stage training strategy, where it first uses MoCo [26] method training on ImageNet dataset, and then trains Kinetics. Our method completely trains from scratch on R2V2, which makes SeCo is not directly comparable to ours.

In order to validate the effectiveness of our method, we conduct ablation study on different loss components with respect to the tracking performance, the results are shown in Table 2. It shows that our proposed $\mathcal{L}_{\text{cycle}}$ clearly improves methods considering only intra-image or intra-video constrative learning. Note that when training with only intra-image invariance without using temporal invariance in videos in R2V2 dataset, the performance for tracking will drop significantly, which is consistent with the results shown in VINCE [21].

4.3. Transfer to image classification

4.3.1 Comparison to state of the art

To further show the generalizability of our method, we transfer the learned representations to perform static image classification task. We use ImageNet dataset [12] to validate our method. We apply one fully-connected layer on frozen representation as linear probing setting in [26, 21]. The results are shown in Table 3. As we could see, our method achieves 55.63% ImageNet Top-1 accuracy, which is 1.23% improvement over VINCE [21], and 2% improvement over MoCo [26] under the same setting, which shows the effectiveness of our proposed method for learning image representation.

4.3.2 Ablation Study

In this section, we design various experiments to show how each of the components of our method affects performance. We use ImageNet, as well as ImageNet-100 dataset [12] as

Methods	Backbone	Dataset	ImageNet
			Top-1 (%)
Supervised	ResNet-50	ImageNet	76.2
MoCo [26]	ResNet-50	ImageNet	67.7
MoCo [26]	ResNet-50	R2V2	53.6
VINCE [21]	ResNet-50	R2V2	54.4
Ours	ResNet-50	R2V2	55.6

Table 3: Linear classification on frozen features results on **ImageNet** compared with other unsupervised representation learning methods.

intra image	Invariance		Backbone	ImageNet Top-1 (%)
	intra video	cross video		
✓			ResNet-18	33.0
✓	✓		ResNet-18	33.1
✓	✓	✓	ResNet-18	34.4
✓			ResNet-50	53.8
✓	✓		ResNet-50	55.1
✓	✓	✓	ResNet-50	55.6

Table 4: Ablation of different losses components ImageNet classification on frozen features. Representations are pretrained on R2V2-S with ResNet-18 and R2V2 with ResNet-50. We clearly see that our proposed method with cross-video cycle consistency learning target achieves the best performance.

our transferring dataset for ablation study, which has 126k train images and 20k test images from 100 classes.

Effect of different loss components. In this part, we study the effect of using different losses to perform unsupervised representation learning and validate the performance on transferring to ImageNet classification. We study three different target of invariance learning, correspond to three loss functions, (a) $\mathcal{L}_{\text{intra-image}}$, (b) $\mathcal{L}_{\text{intra-video}}$, (c) $\mathcal{L} = \mathcal{L}_{\text{intra-video}} + \lambda \mathcal{L}_{\text{cycle}}$ ($\lambda = 0.1$). The unsupervised representation training is performed on R2V2-S (ResNet-18), R2V2 (ResNet-50) dataset. The results are shown in Table 4

As we could see, using a intra-video invariance learning target $\mathcal{L}_{\text{intra-video}}$ improves the ImageNet Top-1 accuracy from 33.0% to 33.1%, indicating that frames within the same video are natural views of the query image. Furthermore, our method, which adds $\mathcal{L}_{\text{cycle}}$ to perform cross-video cycle contrastive learning, further boosts the Top-1 accuracy to 34.4%, which is an absolute 1.4% improvement compared to intra-image invariance learning. With a deeper backbone ResNet-50, a similar trend is observed as the proposed full loss with $\mathcal{L}_{\text{cycle}}$ improves 1.8% Top-1 accuracy over intra-image objective. This shows that adding $\mathcal{L}_{\text{cycle}}$ makes the model explore cross-video relation, making features of visually similar instances across frames and videos closer.

Intra-image or Intra-video invariance are essential for good representation. While exploring cross-image or cross-video information are helping learning better repre-

Size of neighbor set U	128	256	512	16384
Acc Top-1 (%)	56.56	57.00	56.40	52.96
Acc Top-5 (%)	83.10	83.06	82.64	79.46

Table 5: Ablation study. Accuracy on **ImageNet-100** under linear classification protocol varying the size of the neighbor set U . Representations are pretrained **using** $\mathcal{L}_{\text{cycle}}$ **only** on R2V2-S with ResNet-18. One view of the current query image is **included** in the neighbor set.

sation, it should be built on representation that is invariant of instance or videos. We conduct experiments that use $\mathcal{L}_{\text{cycle}}$ only to learn the representation. A random view (data augmentation) k_{++} of the query q_i in the neighbor set U . The results are shown in Table 5. As we could see, when the neighbor size is small (*e.g.* 256), using $\mathcal{L}_{\text{cycle}}$ alone could learn representation that has better performance when transferring to linear classification on ImageNet-100, compared to using $\mathcal{L}_{\text{intra-video}}$. However, when the neighbor set is large, the performance drops largely. On the other hand, if k_{++} is not included in the neighbor set U , using a neighbor size of 256, and $\mathcal{L}_{\text{cycle}}$ alone would lead to 45.78% Top-1 accuracy on ImageNet-100, which is much worse. We safely draw that when neighbor size is small and a random view k_{++} of the query is included in the neighbor set, $\mathcal{L}_{\text{cycle}}$ *degenerates* to $\mathcal{L}_{\text{intra-video}}$ by learning to make the similarity of q_i and k_{++} maximized. Thus, for making the model learn truly cross-video relation, **excluding** k_{++} from the neighbor set U is necessary. However, directly learning correspondence cross videos would be hard and shows worse results of 45.78% Top-1 accuracy on ImageNet-100. It is essential to add $\mathcal{L}_{\text{intra-video}}$ with $\mathcal{L}_{\text{cycle}}$ (*i.e.* using the full loss \mathcal{L} in Eq.), boosting to 58.50 % Top-1 accuracy on ImageNet-100.

How to choose neighbors? We conduct experiments to study how the size of neighbor set U is affecting the performance. Full loss \mathcal{L} is used to perform unsupervised representation learning on R2V2-S dataset and the size of U varies from 256 to 16384. Views of the current query are not added to the neighbor set. Then we evaluate the learned representation by conducting linear classification on froze representation on ImageNet-100. The results are shown in Table 6. As we could see, increasing the neighbor size give us better representation on behalf of better ImageNet-100 Top-1 accuracy. This is expected as a large neighbor size of U would gives higher probability that the query could find correspondence across videos. The best Top-1 accuracy of 58.48% is achieved when using 16384 as neighbor size and we use this as default setting hereafter.

We also study that if using top-K nearest neighbors to perform the reconstruction in Eq. 3 would help representation learning. Top-K neighbors are selected by ranking the similarity $a_{q_i, u}$ in the initial neighbor set, and the top K neighbors are chosen to construct the new neighbor

Size of neighbor set U	256	1024	4096	16384
Acc Top-1 (%)	56.68	57.36	56.82	58.48
Acc Top-5 (%)	84.04	83.78	83.52	83.50

Table 6: Ablation study. Accuracy on **ImageNet-100** under linear classification protocol varying the size of the neighbor set U . Representations are pretrained **using full loss** \mathcal{L} on R2V2-S with ResNet-18.

K	8	16	32	128	256
Acc Top-1 (%)	57.52	57.40	57.64	57.62	56.98
Acc Top-5 (%)	83.02	82.84	83.62	83.76	83.82

Table 7: Ablation study. Accuracy on **ImageNet-100** under linear classification protocol. Ablation on K when using top-K nearest neighbors to perform cross video cycle consistency learning. Representations are pretrained on R2V2-S with ResNet-18.

λ	0.05	0.1	0.3	0.5	0.7	1.0
Acc Top-1 (%)	57.16	58.48	57.04	57.90	57.48	57.84
Acc Top-5 (%)	83.08	83.50	83.80	83.50	83.18	83.70

Table 8: Ablation results on loss balancing factor λ in Eq. 6, Top-1 and Top-5 accuracy results of **ImageNet-100** linear classification on frozen representations are shown. Representations are pretrained on R2V2-S with ResNet-18.

set. Then the cross-video cycle consistency learning is performed using the new neighbor set. Then we transfer the learned representations to the task of linear classification on ImageNet-100. The results are shown in Table 7. We could see that the top-1 accuracy is robust of a wide range of K, from 8 to 128. However, using top-K neighbors show worse performance compared to randomly chosen a neighbor set U of size 16384, which has 58.50% Top-1 accuracy on ImageNet-100. We conjecture that a large and random neighbor set could have higher probability of finding visual similar images and could correct the model’s false belief at early stage that misses useful neighbors in the top-K neighbors. Thus we randomly choose the neighbors U and set the size of U to 16384 as default.

Balance between intra-video invariance and cross-video relation learning. We study the influence of the balancing factor λ in the loss term \mathcal{L} . We conduct unsupervised representation learning using different balancing factor λ in Eq. 6 on R2V2-S dataset, and evaluate the performance using the task of linear classification on frozen learned representation on ImageNet-100 dataset. The results are shown in Table 8. We could see that while adding $\mathcal{L}_{\text{cycle}}$ helps learn better representation for the task of linear classification on ImageNet-100, using a relative small (*e.g.* 0.1) is best. This also coincides our previous finding that intra-video invariance learning $\mathcal{L}_{\text{intra-video}}$ is essential for the cross-video cycle contrast loss $\mathcal{L}_{\text{cycle}}$ to build on. We set $\lambda = 0.1$ as default hereafter.

4.4. Transfer to video action recognition

4.4.1 Comparison to state of the art

We evaluate the learned feature representation on the task of video action recognition on UCF101 [54] dataset. UCF101 has 13320 videos from 101 action categories. We train and test our model on split1 of UCF101. For simplicity, we directly use ResNet other than 3D convolution based methods. The video representation is obtained by averaging the frame representation from the video, and one fully-connected layer is used for predicting the action class on this video representation. Following [42], multiple clips are sampled from the video and the predictions of the clips are averaged for the final results. The results are shown in Table 9. As we could see, our method is able to achieve 76.8% top-1 accuracy on UCF101 with ResNet-18 as backbone, surpassing the previous best one of 68.2% with similar number of parameters.

We also list some results of methods with large 3D ConvNets models in Table 9. Our method is not directly comparable to these methods as we use 2D ConvNets, which not only have less parameters but also much less FLOPs compared to 3D ConvNets. We emphasize that our representation is able to solve multiple downstream tasks while the previous 3D ConvNets are designed only for action recognition. Note that, while DPC with large 3D-ResNet34 (32.6M) as backbone achieves 75.7%, our model with fewer parameters (11.7M), is able to surpass DPC with 3D-ResNet18 (14.2M) as backbone. Notably, when using ResNet-50 as backbone, our method is able to achieve 82.1%, surpassing other methods with larger 3D ConvNets models (*e.g.* MemDPC) as well. The results validate the effectiveness and transferability of the learned representations of our method.

4.4.2 Ablation Study

We study the effect of different losses on the task of video action recognition on UCF-100 dataset. The pre-trained representations are fixed and a single fully-connected layer is added to predict the action class upon the averaged frame representations. The results are shown in Table 10. As we could see, for video action recognition task, it is beneficial to learn representations that are invariant within the same video, compared to invariant to the same image, rises the Top-1 accuracy from 45.1% to 48.4%, with ResNet-18 as backbone. However, it is also beneficial to make representations of similar videos closer other than separating them, as adding our cross-video cycle-contrastive learning loss $\mathcal{L}_{\text{cycle}}$ further improves the Top-1 accuracy to 50.5%. Similarly, when using ResNet-50 as backbone, adding our $\mathcal{L}_{\text{cycle}}$ achieves the best results of 67.1%. The results validate that our proposed cross-video cycle-contrastive learning target

Method	Backbone	#Param	Dataset	UCF101
Random Initialization [24]	3D-ResNet18	14.2M	-	46.5
ImageNet Supervised Pretrained [53]	VGG-M-2048	353M	-	73.0
Shuffle & Learn [41] (227 × 227)	AlexNet	61M	UCF101/HMDB51	50.2
OPN [39]	AlexNet	61M	UCF101	56.3
DPC [24](128 × 128)	3D-ResNet18	14.2M	UCF101	60.6
3D-RotNet [35] (112 × 112)	3D-ResNet18-full	33.6M	Kinetics-400	62.9
3D-ST-Puzzle [36] (224 × 224)	3D-ResNet18-full	33.6M	Kinetics-400	63.9
SpeedNet [5] (224 × 224)	I3D	12.1M	Kinetics-400	66.7
DPC [24](128 × 128)	3D-ResNet18	14.2M	Kinetics-400	68.2
DPC [24](224 × 224)	3D-ResNet34	-	Kinetics-400	75.7
Video-Pace [58]	R(2+1)D	33.3M	Kinetics-400	77.1
CBT [55] (112x112)	S3D	-	Kinetics-400	79.5
MemDPC [25]	R-2D3D	32.4M	Kinetics-400	78.1
Temporal-ssl [34]	R(2+1)D	33.3M	Kinetics-400	81.6
VTHCL [69]	3D-ResNet50	31.7M	Kinetics-400	82.1
Ours(224 × 224)	ResNet-18	11.69 M	R2V2	76.8
Ours(224 × 224)	ResNet-50	25.56 M	R2V2	82.1
XDC [2] (224x224)	R(2+1)D	33.3M	Kinetics-400	86.8
AVID+CMA [42](224x224)	R(2+1)D	33.3M	Kinetics-400	87.5
CVRL [50]	3D-ResNet50	31.7M	Kinetics-400	92.9
ρ BYOL [18]	3D-ResNet50	31.8M	Kinetics-400	95.5

Table 9: Video action recognition accuracy comparison with other unsupervised representation methods on UCF101. We compare with methods using RGB modality. We mainly compare with models that has **similar parameters** as ours and list some large 3D ConvNet models (in gray) for reference.

intra image	Invariance		Backbone	UCF101 Top-1 (%)
	intra video	cross video		
✓			ResNet-18	45.1
✓	✓		ResNet-18	48.4
✓	✓	✓	ResNet-18	50.5
✓			ResNet-50	62.2
✓	✓		ResNet-50	66.2
✓	✓	✓	ResNet-50	67.1

Table 10: Ablation of different losses components UCF action recognition learned on frozen features. Representations are pre-trained on R2V2 with ResNet-18 and ResNet-50.

can learn representations that transfer well to video recognition tasks.

4.4.3 Nearest Neighbor evaluation

To further validate our representation could learn cross-video information, we perform nearest neighbor retrieval experiments on the learned representation on UCF101 dataset on both frame level and clip level.

For frame retrieval experiments, following [7], 10 frames are sampled for each video. The representations of the frames from test set are used to find the nearest neighbors on the train set. For clip retrieval experiments, following [67], 10 clips per video are sampled. The clips extracted from the test set are used to find nearest neighbors on the train set. Cosine distance of representations is used as ranking criterion. If the class of the query sample appears in the class

set of the k nearest neighbors, it is considered as a correct retrieval.

The results are shown in Table 11. Our model is able to surpass previous methods largely on both frame retrieval and clip retrieval experiments. Notably, our method with ResNet-18 as backbone has a superior accuracy when considering small k (e.g. $k=1, 5, 10$). For instance, our method achieves a top-1 accuracy of 45.8% on frame retrieval experiments, where previous best result from Buchler *et al.* [7] is 25.7%, which is an absolute 20.1% improvement. For clip retrieval, our method has a top-1 accuracy of 39.7%, an absolute 25.6% improvement compared to previous best of 14.1%. This indicates that our method is able to make the representations of similar frames/videos (short clips) closer, as they have higher probability belonging to the same class. Furthermore, our model is trained solely on R2V2 dataset and has never seen samples from UCF101 dataset, while other methods is trained on UCF101. The results indicate the transferability of our method. Video representations are obtained by averaging clip representations. We could see that even though our model does not have ground truth class to guide the representation learning, it manages to make video representations from the same class or having similar visual structures close.

Overall, we design various ablation experiments to study different components of the loss, including image recognition, video recognition, video retrieval, tracking. The results validate the effectiveness of our proposed cross-video cycle-contrastive learning target loss $\mathcal{L}_{\text{cycle}}$.

Methods	Training Data	Top-1	Top-5	Top-10	Top-20	Top-50
<i>Frame retrieval:</i>						
Jigsaw [43](CaffeNet)	ImageNet	19.7	28.5	33.5	40.0	49.4
OPN [39](CaffeNet)	UCF101	19.9	28.7	34.0	40.6	51.6
Buchler [7](CaffeNet)	ImageNet+UCF101	25.7	36.2	42.2	49.2	59.5
Ours (ResNet-18)	R2V2	45.8	56.2	61.4	67.0	75.2
Ours (ResNet-50)	R2V2	52.6	63.3	68.1	73.3	80.6
<i>Clip retrieval:</i>						
Order [67] (C3D)	UCF101	12.5	29.0	39.0	50.6	66.9
Order [67] (R(2+1)D)	UCF101	10.7	25.9	35.4	47.3	63.9
Order [67] (R3D)	UCF101	14.1	30.3	40.0	51.1	66.5
SpeedNet [5] (S3D-G)	Kinetics-400	13.0	28.1	37.5	49.5	65.0
Ours (ResNet-18)	R2V2	39.7	50.3	55.9	62.0	70.7
Ours (ResNet-50)	R2V2	46.8	56.7	62.1	67.6	75.1

Table 11: Frame retrieval and Clip retrieval results on **UCF101** compared to other unsupervised representation learning methods. Results of Jigsaw and OPN are taken from [7]. Our model largely surpasses previous methods and manages to do so without using UCF101 samples.

5. Conclusion

In this paper, we propose a cross-video cycle-consistent contrastive learning objective to perform self-supervised learning for image representations. The proposed method could learn to explore cross-video relations to make not only the representations of images within the same video closer, but also representations from different videos with similar visual structures close, without using ground truth class labels or generating pseudo labels. We perform self-supervised representation learning on unlabeled R2V2 video dataset, and show that the learned image representation transfer well to multiple downstream tasks including visual tracking, image classification and action recognition. Extensive ablation studies are conducted and validate the effectiveness of our proposed method. We hope our approach can open up an opportunity to utilize cross-instance paired data for learning general image representations.

References

- [1] Pulkit Agrawal, Joao Carreira, and Jitendra Malik. Learning to see by moving. In *ICCV*, 2015. 2
- [2] Humam Alwassel, Dhruv Mahajan, Bruno Korbar, Lorenzo Torresani, Bernard Ghanem, and Du Tran. Self-supervised learning by cross-modal audio-video clustering. *arXiv preprint arXiv:1911.12667*, 2019. 8
- [3] Philip Bachman, R Devon Hjelm, and William Buchwalter. Learning representations by maximizing mutual information across views. In *Advances in Neural Information Processing Systems*, pages 15535–15545, 2019. 1, 2
- [4] Aayush Bansal, Shugao Ma, Deva Ramanan, and Yaser Sheikh. Recycle-gan: Unsupervised video retargeting. In *ECCV*, 2018. 2
- [5] Sagie Benaim, Ariel Ephrat, Oran Lang, Inbar Mosseri, William T Freeman, Michael Rubinstein, Michal Irani, and Tali Dekel. Speednet: Learning the speediness in videos. In *Proceedings of the IEEE/CVF Conference on Computer Vision and Pattern Recognition*, pages 9922–9931, 2020. 2, 8, 9
- [6] Luca Bertinetto, Jack Valmadre, Joao F Henriques, Andrea Vedaldi, and Philip HS Torr. Fully-convolutional siamese networks for object tracking. In *European conference on computer vision*, pages 850–865. Springer, 2016. 5
- [7] Uta Buchler, Biagio Brattoli, and Bjorn Ommer. Improving spatiotemporal self-supervision by deep reinforcement learning. In *Proceedings of the European conference on computer vision (ECCV)*, pages 770–786, 2018. 2, 8, 9
- [8] Mathilde Caron, Ishan Misra, Julien Mairal, Priya Goyal, Piotr Bojanowski, and Armand Joulin. Unsupervised learning of visual features by contrasting cluster assignments. In *Advances in Neural Information Processing Systems*, pages 9912–9924, 2020. 2
- [9] Ting Chen, Simon Kornblith, Mohammad Norouzi, and Geoffrey Hinton. A simple framework for contrastive learning of visual representations. *arXiv preprint arXiv:2002.05709*, 2020. 1, 2, 3
- [10] Xinlei Chen, Haoqi Fan, Ross Girshick, and Kaiming He. Improved baselines with momentum contrastive learning. *arXiv preprint arXiv:2003.04297*, 2020. 2
- [11] Xinlei Chen and Kaiming He. Exploring simple siamese representation learning. *arXiv preprint arXiv:2011.10566*, 2020. 5
- [12] Jia Deng, Wei Dong, Richard Socher, Li-Jia Li, Kai Li, and Li Fei-Fei. Imagenet: A large-scale hierarchical image database. In *2009 IEEE conference on computer vision and pattern recognition*, pages 248–255. Ieee, 2009. 5
- [13] Carl Doersch, Abhinav Gupta, and Alexei A Efros. Unsupervised visual representation learning by context prediction. In *Proceedings of the IEEE international conference on computer vision*, pages 1422–1430, 2015. 2
- [14] Jeff Donahue, Philipp Krähenbühl, and Trevor Darrell. Adversarial feature learning. *arXiv preprint arXiv:1605.09782*, 2016. 2

- [15] Alexey Dosovitskiy, Philipp Fischer, Jost Tobias Springenberg, Martin Riedmiller, and Thomas Brox. Discriminative unsupervised feature learning with exemplar convolutional neural networks. *IEEE transactions on pattern analysis and machine intelligence*, 38(9):1734–1747, 2015. [2](#)
- [16] Alexey Dosovitskiy, Jost Tobias Springenberg, Martin Riedmiller, and Thomas Brox. Discriminative unsupervised feature learning with convolutional neural networks. In *Advances in neural information processing systems*, pages 766–774, 2014. [2](#)
- [17] Debidatta Dwibedi, Yusuf Aytar, Jonathan Tompson, Pierre Sermanet, and Andrew Zisserman. Temporal cycle-consistency learning. In *Proceedings of the IEEE Conference on Computer Vision and Pattern Recognition*, pages 1801–1810, 2019. [2](#)
- [18] Christoph Feichtenhofer, Haoqi Fan, Bo Xiong, Ross Girshick, and Kaiming He. A large-scale study on unsupervised spatiotemporal representation learning. *arXiv preprint arXiv:2104.14558*, 2021. [8](#)
- [19] Spyros Gidaris, Praveer Singh, and Nikos Komodakis. Unsupervised representation learning by predicting image rotations. *arXiv preprint arXiv:1803.07728*, 2018. [2](#)
- [20] Clément Godard, Oisín Mac Aodha, and Gabriel J Brostow. Unsupervised monocular depth estimation with left-right consistency. 2017. [2](#)
- [21] Daniel Gordon, Kiana Ehsani, Dieter Fox, and Ali Farhadi. Watching the world go by: Representation learning from unlabeled videos. *arXiv preprint arXiv:2003.07990*, 2020. [1](#), [2](#), [3](#), [4](#), [5](#), [6](#)
- [22] Ross Goroshin, Joan Bruna, Jonathan Tompson, David Eigen, and Yann LeCun. Unsupervised learning of spatiotemporally coherent metrics. *ICCV*, 2015. [2](#)
- [23] Raia Hadsell, Sumit Chopra, and Yann LeCun. Dimensionality reduction by learning an invariant mapping. In *2006 IEEE Computer Society Conference on Computer Vision and Pattern Recognition (CVPR'06)*, volume 2, pages 1735–1742. IEEE, 2006. [2](#)
- [24] Tengda Han, Weidi Xie, and Andrew Zisserman. Video representation learning by dense predictive coding. In *Proceedings of the IEEE International Conference on Computer Vision Workshops*, pages 0–0, 2019. [2](#), [8](#)
- [25] Tengda Han, Weidi Xie, and Andrew Zisserman. Memory-augmented dense predictive coding for video representation learning. *arXiv preprint arXiv:2008.01065*, 2020. [2](#), [8](#)
- [26] Kaiming He, Haoqi Fan, Yuxin Wu, Saining Xie, and Ross Girshick. Momentum contrast for unsupervised visual representation learning. In *Proceedings of the IEEE/CVF Conference on Computer Vision and Pattern Recognition*, pages 9729–9738, 2020. [1](#), [2](#), [3](#), [4](#), [5](#), [6](#)
- [27] Kaiming He, Xiangyu Zhang, Shaoqing Ren, and Jian Sun. Deep residual learning for image recognition. In *Proceedings of the IEEE conference on computer vision and pattern recognition*, pages 770–778, 2016. [4](#), [5](#)
- [28] Olivier J Hénaff, Aravind Srinivas, Jeffrey De Fauw, Ali Razavi, Carl Doersch, SM Eslami, and Aaron van den Oord. Data-efficient image recognition with contrastive predictive coding. *arXiv preprint arXiv:1905.09272*, 2019. [1](#), [2](#)
- [29] R Devon Hjelm, Alex Fedorov, Samuel Lavoie-Marchildon, Karan Grewal, Phil Bachman, Adam Trischler, and Yoshua Bengio. Learning deep representations by mutual information estimation and maximization. *arXiv preprint arXiv:1808.06670*, 2018. [1](#), [2](#)
- [30] Lianghua Huang, Xin Zhao, and Kaiqi Huang. Got-10k: A large high-diversity benchmark for generic object tracking in the wild. *IEEE Transactions on Pattern Analysis and Machine Intelligence*, 2019. [5](#)
- [31] Qi-Xing Huang and Leonidas Guibas. Consistent shape maps via semidefinite programming. In *Proceedings of the Eleventh Eurographics/ACMSIGGRAPH Symposium on Geometry Processing*, 2013. [2](#)
- [32] Allan Jabri, Andrew Owens, and Alexei Efros. Space-time correspondence as a contrastive random walk. In *Advances in Neural Information Processing Systems*, pages 19545–19560, 2020. [2](#)
- [33] Dinesh Jayaraman and Kristen Grauman. Learning image representations tied to ego-motion. In *Proceedings of the IEEE International Conference on Computer Vision*, pages 1413–1421, 2015. [2](#)
- [34] Simon Jenni, Givi Meishvili, and Paolo Favaro. Video representation learning by recognizing temporal transformations. *arXiv preprint arXiv:2007.10730*, 2020. [2](#), [8](#)
- [35] Longlong Jing and Yingli Tian. Self-supervised spatiotemporal feature learning by video geometric transformations. *arXiv preprint arXiv:1811.11387*, 2(7):8, 2018. [2](#), [8](#)
- [36] Dahun Kim, Donghyeon Cho, and In So Kweon. Self-supervised video representation learning with space-time cubic puzzles. In *Proceedings of the AAAI Conference on Artificial Intelligence*, volume 33, pages 8545–8552, 2019. [2](#), [8](#)
- [37] Quan Kong, Wenpeng Wei, Ziwei Deng, Tomoaki Yoshinaga, and Tomokazu Murakami. Cycle-contrast for self-supervised video representation learning. *arXiv preprint arXiv:2010.14810*, 2020. [2](#)
- [38] Zihang Lai and Weidi Xie. Self-supervised learning for video correspondence flow. *arXiv preprint arXiv:1905.00875*, 2019. [2](#)
- [39] Hsin-Ying Lee, Jia-Bin Huang, Maneesh Singh, and Ming-Hsuan Yang. Unsupervised representation learning by sorting sequences. In *Proceedings of the IEEE International Conference on Computer Vision*, pages 667–676, 2017. [2](#), [8](#), [9](#)
- [40] Ishan Misra and Laurens van der Maaten. Self-supervised learning of pretext-invariant representations. In *Proceedings of the IEEE/CVF Conference on Computer Vision and Pattern Recognition*, pages 6707–6717, 2020. [1](#), [2](#)
- [41] Ishan Misra, C Lawrence Zitnick, and Martial Hebert. Shuffle and learn: unsupervised learning using temporal order verification. In *European Conference on Computer Vision*, pages 527–544. Springer, 2016. [2](#), [8](#)
- [42] Pedro Morgado, Nuno Vasconcelos, and Ishan Misra. Audio-visual instance discrimination with cross-modal agreement. 2020. [2](#), [7](#), [8](#)
- [43] Mehdi Noroozi and Paolo Favaro. Unsupervised learning of visual representations by solving jigsaw puzzles. In

- European Conference on Computer Vision*, pages 69–84. Springer, 2016. 9
- [44] Aaron van den Oord, Yazhe Li, and Oriol Vinyals. Representation learning with contrastive predictive coding. *arXiv preprint arXiv:1807.03748*, 2018. 2
- [45] Andrew Owens, Jiajun Wu, Josh H McDermott, William T Freeman, and Antonio Torralba. Ambient sound provides supervision for visual learning. In *European conference on computer vision*, pages 801–816. Springer, 2016. 2
- [46] Deepak Pathak, Ross Girshick, Piotr Dollár, Trevor Darrell, and Bharath Hariharan. Learning features by watching objects move. In *Proceedings of the IEEE Conference on Computer Vision and Pattern Recognition*, pages 2701–2710, 2017. 2
- [47] Deepak Pathak, Philipp Krahenbuhl, Jeff Donahue, Trevor Darrell, and Alexei A Efros. Context encoders: Feature learning by inpainting. In *Proceedings of the IEEE conference on computer vision and pattern recognition*, pages 2536–2544, 2016. 2
- [48] Senthil Purushwalkam and Abhinav Gupta. Demystifying contrastive self-supervised learning: Invariances, augmentations and dataset biases. *arXiv preprint arXiv:2007.13916*, 2020. 1, 2, 3
- [49] Senthil Purushwalkam, Tian Ye, Saurabh Gupta, and Abhinav Gupta. Aligning videos in space and time. In *European Conference on Computer Vision*, pages 262–278. Springer, 2020. 2
- [50] Rui Qian, Tianjian Meng, Boqing Gong, Ming-Hsuan Yang, Huisheng Wang, Serge Belongie, and Yin Cui. Spatiotemporal contrastive video representation learning. *arXiv preprint arXiv:2008.03800*, 2020. 2, 8
- [51] Nawid Sayed, Biagio Brattoli, and Björn Ommer. Cross and learn: Cross-modal self-supervision. In *German Conference on Pattern Recognition*, pages 228–243. Springer, 2018. 2
- [52] Pierre Sermanet, Corey Lynch, Yevgen Chebotar, Jasmine Hsu, Eric Jang, Stefan Schaal, Sergey Levine, and Google Brain. Time-contrastive networks: Self-supervised learning from video. In *2018 IEEE International Conference on Robotics and Automation (ICRA)*, pages 1134–1141. IEEE, 2018. 3
- [53] Karen Simonyan and Andrew Zisserman. Two-stream convolutional networks for action recognition in videos. In *Advances in neural information processing systems*, pages 568–576, 2014. 8
- [54] Khurram Soomro, Amir Roshan Zamir, and Mubarak Shah. Ucf101: A dataset of 101 human actions classes from videos in the wild. *arXiv preprint arXiv:1212.0402*, 2012. 7
- [55] Chen Sun, Fabien Baradel, Kevin Murphy, and Cordelia Schmid. Learning video representations using contrastive bidirectional transformer. *arXiv preprint arXiv:1906.05743*, 2019. 8
- [56] Yonglong Tian, Dilip Krishnan, and Phillip Isola. Contrastive multiview coding. *arXiv preprint arXiv:1906.05849*, 2019. 1, 2
- [57] Yonglong Tian, Chen Sun, Ben Poole, Dilip Krishnan, Cordelia Schmid, and Phillip Isola. What makes for good views for contrastive learning. *arXiv preprint arXiv:2005.10243*, 2020. 1
- [58] Jiangliu Wang, Jianbo Jiao, and Yun-Hui Liu. Self-supervised video representation learning by pace prediction. In *European Conference on Computer Vision*, pages 504–521. Springer, 2020. 2, 8
- [59] Ning Wang, Yibing Song, Chao Ma, Wengang Zhou, Wei Liu, and Houqiang Li. Unsupervised deep tracking. In *Proceedings of the IEEE/CVF Conference on Computer Vision and Pattern Recognition*, pages 1308–1317, 2019. 2
- [60] Xiaolong Wang and Abhinav Gupta. Unsupervised learning of visual representations using videos. In *ICCV*, 2015. 1, 2
- [61] Xiaolong Wang, Kaiming He, and Abhinav Gupta. Transitive invariance for self-supervised visual representation learning. In *Proceedings of the IEEE international conference on computer vision*, pages 1329–1338, 2017. 2
- [62] Xiaolong Wang, Allan Jabri, and Alexei A Efros. Learning correspondence from the cycle-consistency of time. In *Proceedings of the IEEE Conference on Computer Vision and Pattern Recognition*, pages 2566–2576, 2019. 2
- [63] Donglai Wei, Joseph J Lim, Andrew Zisserman, and William T Freeman. Learning and using the arrow of time. In *Proceedings of the IEEE Conference on Computer Vision and Pattern Recognition*, pages 8052–8060, 2018. 2
- [64] Yi Wu, Jongwoo Lim, and Ming-Hsuan Yang. Online object tracking: A benchmark. In *Proceedings of the IEEE conference on computer vision and pattern recognition*, pages 2411–2418, 2013. 5
- [65] Zhirong Wu, Yuanjun Xiong, Stella X Yu, and Dahua Lin. Unsupervised feature learning via non-parametric instance discrimination. In *Proceedings of the IEEE Conference on Computer Vision and Pattern Recognition*, pages 3733–3742, 2018. 1, 2
- [66] Tete Xiao, Xiaolong Wang, Alexei A Efros, and Trevor Darrell. What should not be contrastive in contrastive learning. *arXiv preprint arXiv:2008.05659*, 2020. 1, 5
- [67] Dejing Xu, Jun Xiao, Zhou Zhao, Jian Shao, Di Xie, and Yueting Zhuang. Self-supervised spatiotemporal learning via video clip order prediction. In *Proceedings of the IEEE Conference on Computer Vision and Pattern Recognition*, pages 10334–10343, 2019. 8, 9
- [68] Jiarui Xu and Xiaolong Wang. Rethinking self-supervised correspondence learning: A video frame-level similarity perspective. *arXiv preprint arXiv:2103.17263*, 2021. 2
- [69] Ceyuan Yang, Yinghao Xu, Bo Dai, and Bolei Zhou. Video representation learning with visual tempo consistency. *arXiv preprint arXiv:2006.15489*, 2020. 8
- [70] Ting Yao, Yiheng Zhang, Zhaofan Qiu, Yingwei Pan, and Tao Mei. Seco: Exploring sequence supervision for unsupervised representation learning. *arXiv preprint arXiv:2008.00975*, 2020. 5
- [71] Zhichao Yin and Jianping Shi. Geonet: Unsupervised learning of dense depth, optical flow and camera pose. In *CVPR*, 2018. 2
- [72] Richard Zhang, Phillip Isola, and Alexei A Efros. Colorful image colorization. In *European conference on computer vision*, pages 649–666. Springer, 2016. 2
- [73] Tinghui Zhou, Matthew Brown, Noah Snavely, and David G Lowe. Unsupervised learning of depth and ego-motion from video. In *CVPR*, 2017. 2

- [74] Tinghui Zhou, Yong Jae Lee, Stella X Yu, and Alyosha A Efros. Flowweb: Joint image set alignment by weaving consistent, pixel-wise correspondences. In *CVPR*, 2015. 2
- [75] Tinghui Zhou, Philipp Krahenbuhl, Mathieu Aubry, Qixing Huang, and Alexei A Efros. Learning dense correspondence via 3d-guided cycle consistency. In *Proceedings of the IEEE Conference on Computer Vision and Pattern Recognition*, pages 117–126, 2016. 2
- [76] Xiaowei Zhou, Menglong Zhu, and Kostas Daniilidis. Multi-image matching via fast alternating minimization. In *ICCV*, 2015. 2
- [77] Jun-Yan Zhu, Taesung Park, Phillip Isola, and Alexei A Efros. Unpaired image-to-image translation using cycle-consistent adversarial networks. In *Proceedings of the IEEE international conference on computer vision*, pages 2223–2232, 2017. 2
- [78] Chengxu Zhuang, Alex Lin Zhai, and Daniel Yamins. Local aggregation for unsupervised learning of visual embeddings. In *Proceedings of the IEEE International Conference on Computer Vision*, pages 6002–6012, 2019. 2